

Future projections of ecological patterns in the Baltic Sea

H.E.M. Meier and K. Eilola

Swedish Meteorological and Hydrological Institute, Department of Research and Development, Norrköping, Sweden

Abstract. The impact of changing climate on Baltic Sea biogeochemical cycles at the end of the 21st century was studied using a three-dimensional coupled physical-biogeochemical model. Four climate change scenarios using regionalized data from two General Circulation Models (GCMs) and two greenhouse gas emission scenarios (A2, B2) have been investigated. In this study we have focused on maps of annual and seasonal mean changes of ecological quality indicators. We found that the impact of changing climate on the horizontal distribution of ecological parameters might be significant. For instance, in the scenario simulation with the largest changes secchi depth might decrease by up to 2 m in some regions. However, due to reduced stratification also increased secchi depths might occur.

1. Introduction

The AMBER project (Assessment and Modelling Baltic Ecosystem Response) aims to implement and to apply the Ecosystem Approach to Management (EAM) to the Baltic Sea with a focus on the coastal ecosystem (<http://www.io-warnemuende.de/amber.html>). Within AMBER models are applied for future projections applying the ensemble approach to reduce model uncertainties. The resulting projections are important contributions for the development of EAM tools.

According to the AMBER science plan the most important goals of AMBER are (see the AMBER homepage):

- “Qualitative risk assessments for various climate change scenarios, land uses and life style change scenarios.”
 - “Derivation of mitigation strategies from the risk assessment. Mitigation strategies are necessary tools for integrated management.”
 - “Development of Ecological Quality Objectives (EcoQOs) for the application of EAM following the guidance of ICES (2005). EcoQOs are a basis for”
 - “the development of indicators, limits and targets. These quantitatively describe ecosystem state, ecosystem properties or impacts. Finally, cost-effective indicators will be developed to improve monitoring strategies and to guide environmental management in decision making.”
- “EAM with its tools risk assessment, mitigation strategies, derivation of EcoQOs and improve-

ment of monitoring strategies will be the core of science based advice for integrated management.”

In this report, results of an ensemble of scenario simulations are described assuming present nutrient concentrations for the calculation of nutrient loads from land. These results will contribute to the EAM tool to be developed within AMBER. In the next section the method of the dynamical downscaling approach and the models are briefly introduced. In the third section results of annual and seasonal mean changes of 12 key parameters including ecological quality indicators like sea surface temperature, sea surface salinity, bottom salinity, sea surface height, bottom oxygen concentration, surface layer phosphate concentration, surface layer nitrate concentration, surface layer diatom concentration, surface layer concentration of flagellates and others, surface layer cyanobacteria concentration, surface layer phytoplankton concentration, and secchi depth are presented and discussed. Finally, the main findings are summarized.

2. Method

We have used the three-dimensional circulation model RCO, the Rossby Centre Ocean model. RCO is a Bryan-Cox-Semtner primitive equation circulation model with a free surface and open boundary conditions in the northern Kattegat. In case of inflow prognostic variables like temperature, salinity and nutrients are nudged towards climatologically annual mean profiles calculated from observations. In case of outflow a Orlandi radiation condition is used. RCO is coupled to a Hibler-type sea ice model with elastic-viscous-plastic

rheology. Subgrid-scale vertical mixing is parameterized using a turbulence closure scheme of the k-e type. In the present study, RCO was used with a horizontal resolution of 11.1 km (6 nautical miles) and with 42 vertical levels with layer thicknesses ranging between 3 m in the surface layer and 12 m in the deepest layer. A flux-corrected, monotonicity preserving transport (FCT) scheme is embedded and no explicit horizontal diffusion is applied. For further details of the RCO model the reader is referred to *Meier et al.* [2003].

The Swedish Coastal and Ocean Biogeochemical model (SCOBI) is coupled to the physical model RCO. SCOBI describes the dynamics of nitrate, ammonium, phosphate, phytoplankton, zooplankton, detritus, and oxygen. Here, phytoplankton consists of three algal groups representing diatoms, flagellates and others, and cyanobacteria. Besides the possibility to assimilate inorganic nutrients the modelled cyanobacteria also has the ability to fix molecular nitrogen which may constitute an external nitrogen source for the model system. The sediment contains nutrients in the form of benthic nitrogen and benthic phosphorus including aggregated process descriptions for oxygen dependent nutrient regeneration, denitrification and adsorption of ammonium to sediment particles, as well as permanent burial of organic matter. For further details of the SCOBI model description the reader is referred to *Eilola et al.* [2009].

Four scenario simulations have been performed. The forcing was calculated applying a dynamical downscaling approach using a regional climate model (RCM) with lateral boundary data from two General Circulation Models (GCMs). The two GCMs used were HadAM3H from the Hadley Centre in the U.K. and ECHAM4/OPYC3 from the Max Planck Institute for Meteorology in Germany. For each of these two driving global models scenario simulations forced with either the A2 or the B2 emission scenario were conducted. The future projections refer to a period at the end of this century (2070-2099). Thereby the so-called delta approach was applied. In this approach it is assumed that only the mean seasonal cycle will change whereas the variability in time is assumed to be the same as during the control period 1969-1998. For further details of the method and results of the scenario simulations the reader is referred to *Meier et al.* [2011a].

3. Results and Discussion

Annual and seasonal mean changes of the 12 selected parameters between the periods 2070-2099 and 1969-1998 are depicted in Figures 1 to 12.

We found larger sea surface temperature (SST) changes in the A2 than in the B2 scenarios (Fig. 1). In all four scenario simulations largest SST changes occur in the northern Baltic Sea (Bothnian Sea and Bothnian Bay) during summer. These results are explained by the sea-

ice - albedo feedback [*Meier et al.*, 2011b]. The warming is larger in the center of the Bothnian Sea and Bothnian Bay than in the coastal zone. In ECHAM4/OPYC3 driven scenario simulations large warming signals are also found in the Baltic proper during spring.

Changes of the sea surface salinity (SSS) and bottom salinity are controlled by changing wind fields and by changing freshwater supply from land [*Meier*, 2006] (Figs. 2 and 3). In HadAM3H driven scenario simulations SSSs and bottom salinities decrease only slightly by about 0.5. These changes are within the range of present natural variability [*Meier et al.*, 2006]. To the contrary, in ECHAM4/OPYC3 driven scenario simulations both increased winter mean wind speed and increased annual mean runoff affect salinity significantly [*Meier et al.*, 2006]. Largest SSS changes of up to more than 3 were found in the northern Baltic proper. Largest bottom salinity changes of up to more than 5 were found in the western Gulf of Finland.

In Figure 4 changes of sea surface height (SSH) are related to changes of the regional wind patterns. In the presented scenario simulations changes of eustatic sea level rise and land uplift have not been considered (cf. *Meier et al.* [2004]). In ECHAM4/OPYC3 driven scenario simulations the winter mean west wind increases causing SSH changes of more than 20 cm in the Gulf of Finland in the A2 scenario. In HadAM3H driven scenario simulations SSH changes are statistically not significant.

Changes of bottom oxygen concentrations are shown in Figure 5. As the saturation concentration of oxygen is smaller in warmer water bottom oxygen concentrations in the coastal zone without a permanent halocline decrease in all scenario simulations during all seasons. During summer oxygen concentrations are slightly smaller than during winter due to higher water temperatures and due to the consumption of oxygen. However the largest changes are explained by changing hydrographic conditions in the deeper sea areas. Depending on stratification changes bottom oxygen concentrations will change. Increased wind induced mixing and increased runoff cause decreased stratification and an increase of bottom oxygen concentrations. We found largest changes in ECHAM4/OPYC3 driven scenario simulations (Fig. 5).

In ECHAM4/OPYC3 driven scenario simulations surface layer phosphate concentrations decrease following the increasing bottom oxygen concentrations (Fig. 6). As the phosphorus retention capacity of the sediments is highly oxygen dependent the phosphorus concentration in the water column decreases in areas with large changes of the bottom oxygen concentration. Especially in the transition between anoxic and oxic conditions the phosphorus retention capacity is highly dependent of the oxygen concentration. We found largest changes of the surface layer phosphate concentrations in

the southern and eastern Gotland Basin and in the Gulf of Finland. In HadAM3H driven scenario simulations phosphate concentration changes are much smaller except in the area close to the Neva river mouth in the eastern Gulf of Finland.

Also for the distribution changes of nitrate concentrations the changing oxygen concentrations are important. Especially in the oxygen concentration range between 0 and 3 ml l^{-1} is the sensitivity of the denitrification process large. An increase of oxygen concentrations in the water column results in an increase of nitrate concentrations in the surface layer (Fig. 7). In difference to surface layer phosphate concentration changes also the Bothnian Sea is affected by large nitrate concentration changes in the surface layer. In ECHAM4/OPYC3 driven scenario simulations the largest increases of surface layer nitrate concentrations were found in the Gulf of Finland, Gulf of Riga, the northern Gotland Basin and the Bothnian Sea. In HadAM3H driven scenario simulations the corresponding changes are small except in the eastern Gulf of Finland and in the Gulf of Riga.

Concentration changes of diatoms and flagellates and others in the surface layer are largest during spring (Figs. 8 and 9). We found both areas with increased and decreased concentrations. In contrast, concentration changes of cyanobacteria in the surface layer with maxima in summer and autumn are much smaller (Fig. 10). The sum of the concentrations of these three algal groups is the surface layer phytoplankton concentration (Fig. 11). The depicted changes are difficult to understand because changes of water temperature, stratification, light conditions and nutrients as well the ratio of available nitrate and phosphate concentrations in the surface layer are important drivers. Most of the phytoplankton concentration changes are explained by concentration changes of flagellates and others during spring. As suggested by Meier *et al.* [2011a] a key factor explaining the concentration changes of phytoplankton in the scenario simulations is the ratio of available nitrate and phosphate concentrations in the surface layer before the spring bloom, i.e. during winter. Meier *et al.* [2011a] pointed also out that the uncertainty of the simulated changes of cyanobacteria concentrations is mainly related to the parameterization of phosphorus fluxes between the sediments and the water column. As the latter is not well known yet, the uncertainty of the depicted results in Figure 10 might be large.

Factors controlling light attenuation in the Baltic Sea model are the concentrations of yellow substances, phytoplankton and detritus. In the scenario simulations changes of the secchi depth are explained by changing phytoplankton and detritus concentrations because yellow substances are assumed to remain unchanged. The impact of changing phytoplankton concentrations in spring and summer is most obvious in the scenario simulation ECHAM4/OPYC3 A2 (Fig. 12, see also Fig. 11)

where we found secchi depth changes up to 2 m in the Bornholm Basin. However, in other regions with reduced stratification, i.e. in the eastern and northern Gotland Basin, also increased secchi depths are simulated.

4. Summary

Maps of annual and seasonal mean changes of 12 key parameters including important ecological quality indicators have been compiled from results of four scenario simulations for the period 2070-2099 compared to the control period 1969-1998. We found large changes of the horizontal distributions of ecological quality indicators like bottom oxygen concentrations, phytoplankton concentrations and secchi depth. Thus, changing physical conditions like water temperature and stratification have large impacts on the Baltic ecosystem. As the selected scenario simulations are quite different showing large differences in changing physics like increasing water temperatures, wind speeds and freshwater volume flows from land the uncertainty of the simulated ecosystem response is large.

Acknowledgments. The work presented in this study was jointly funded by the Swedish Environmental Protection Agency (SEPA) and the European Commission within the project AMBER (Assessment and Modelling Baltic Ecosystem Response, ref.no. 08/390). AMBER is part of the BONUS+ program (<http://www.bonusportal.org>).

References

- Eilola, K., H. E. M. Meier, and E. Almroth, On the dynamics of oxygen, phosphorus and cyanobacteria in the Baltic Sea; a model study., *J. Marine Systems*, 75, 163–184, 2009.
- Meier, H. E. M., Baltic Sea climate in the late twenty-first century: a dynamical downscaling approach using two global models and two emission scenarios, *Clim. Dyn.*, 2006, published online 11 Apr 2006, doi:10.1007/s00382-006-0124-x.
- Meier, H. E. M., R. Döscher, and T. Faxén, A multiprocessor coupled ice-ocean model for the Baltic Sea: Application to salt inflow, *J. Geophys. Res.*, 108(C8), 3273, doi:10.1029/2000JC000521, 2003.
- Meier, H. E. M., B. Broman, and E. Kjellström, Simulated sea level in past and future climates of the Baltic Sea, *Clim. Res.*, 27, 59–75, 2004.
- Meier, H. E. M., E. Kjellström, and L. P. Graham, Estimating uncertainties of projected Baltic Sea salinity in the late 21st century, *Geophys. Res. Lett.*, 33, L15,705, 2006.
- Meier, H. E. M., K. Eilola, and E. Almroth, Climate-related changes in marine ecosystems simulated with a three-dimensional coupled biogeochemical-physical model of the Baltic Sea, *Clim. Res.*, 2011a, in press.
- Meier, H. E. M., A. Höglund, R. Döscher, H. Andersson, U. Löptien, and E. Kjellström, Quality assessment of atmospheric surface fields over the Baltic Sea of an ensemble of regional climate model simulations with respect to ocean dynamics, *Oceanologia*, 2011b, in press.

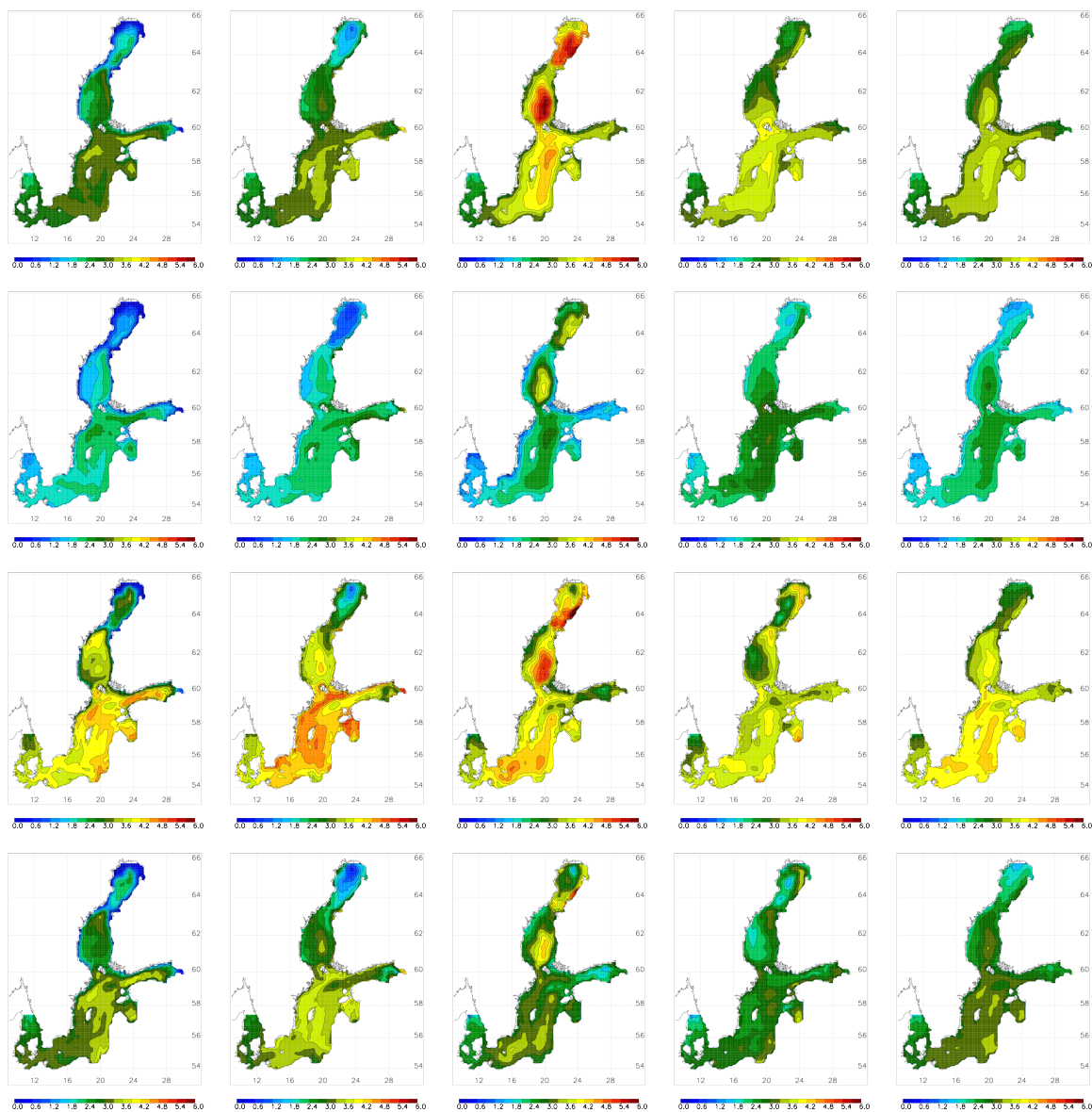


Figure 1. Annual and seasonal mean sea surface temperature (SST) changes (in $^{\circ}\text{C}$) between 2070-2099 and 1969-1998 in RCO-SCOB simulations driven by regionalized GCM results. From left to right results for winter (December through February), spring (March through May), summer (June through August), autumn (September through November) and the annual mean are shown. From top to bottom the following scenario simulations are depicted: RCAO-HADAM3H-A2-REF, RCAO-HADAM3H-B2-REF, RCAO-ECHAM4-A2-REF, RCAO-ECHAM4-B2-REF. Values larger and smaller than the range depicted within the color bar are shown in brown and white, respectively. The color bar covers the range between 0 and 6°C .

H.E.M. Meier and K. Eilola, Swedish Meteorological and Hydrological Institute, Department of Research and Development, SE-60176 Norrköping, Sweden. (e-mail: markus.meier@smhi.se)

This preprint was prepared with AGU's \LaTeX macros v5.01, with the extension package 'AGU++' by P. W. Daly, version 1.6b from 1999/08/19.

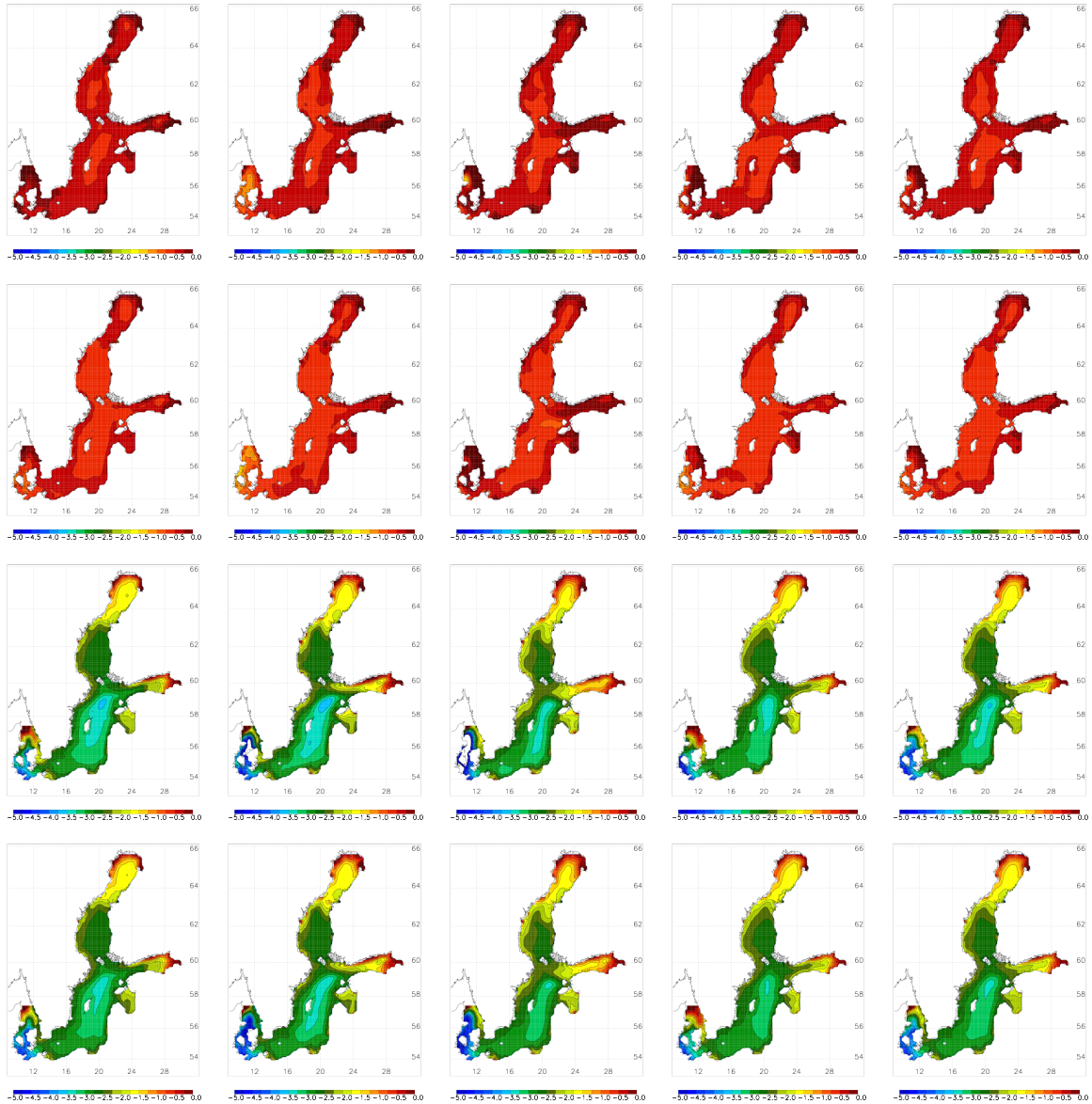


Figure 2. As Figure 1 but for sea surface salinity (SSS) changes. The color bar covers the range between -5 and 0.

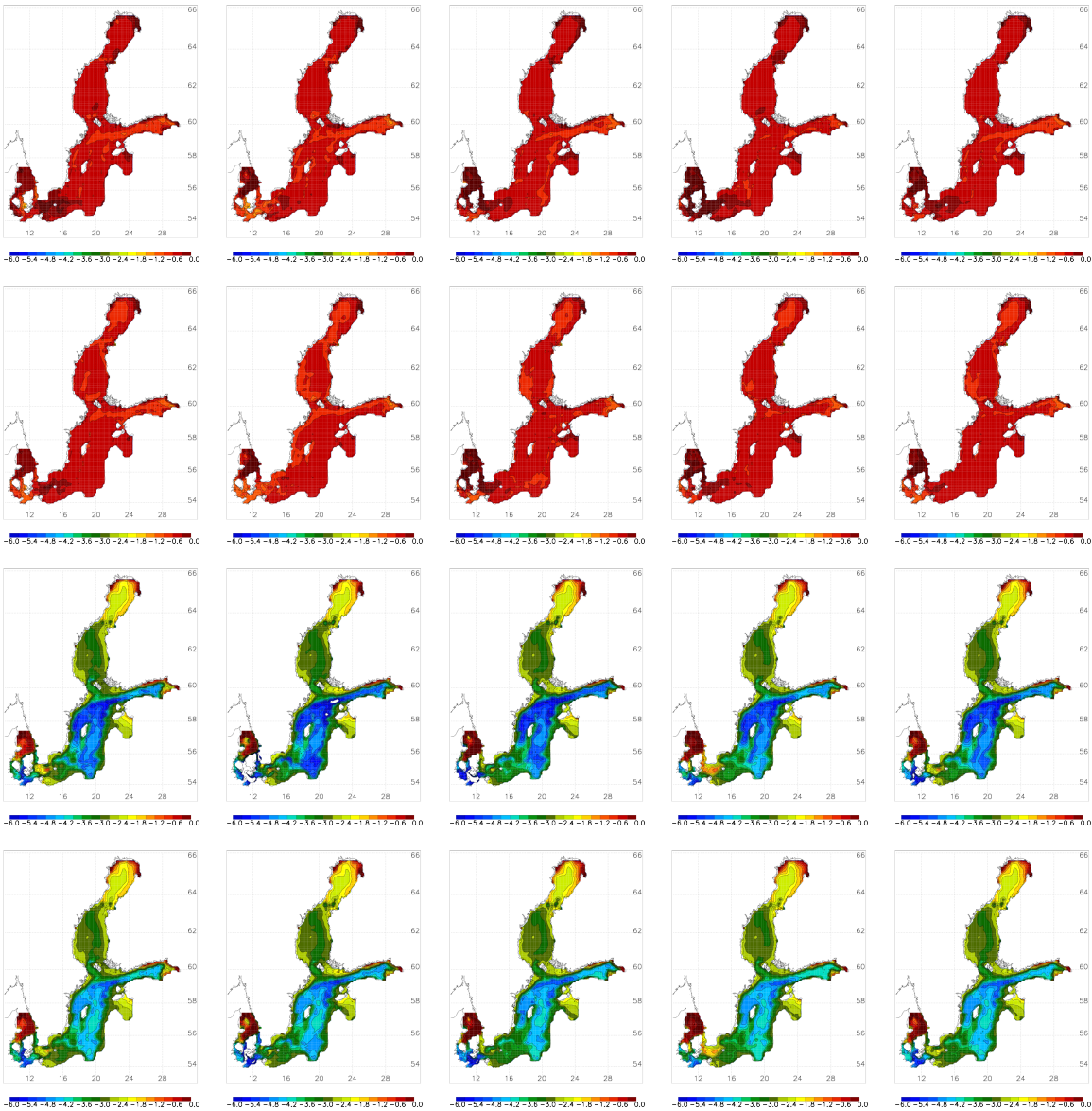


Figure 3. As Figure 1 but for bottom salinity changes. The color bar covers the range between -6 and 0.

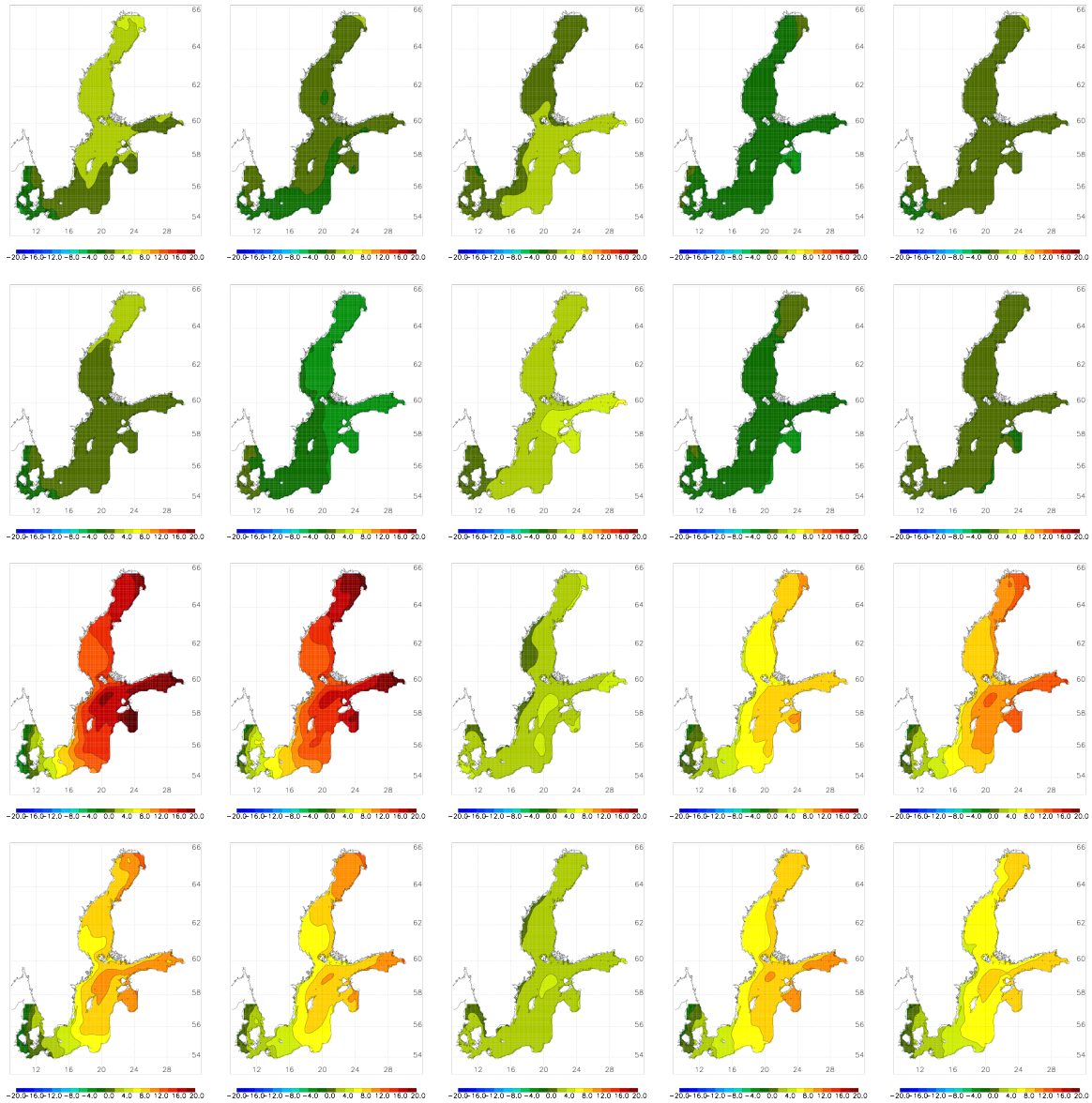


Figure 4. As Figure 1 but for sea surface height (SSH) changes (in cm). The color bar covers the range between -20 and +20 cm.

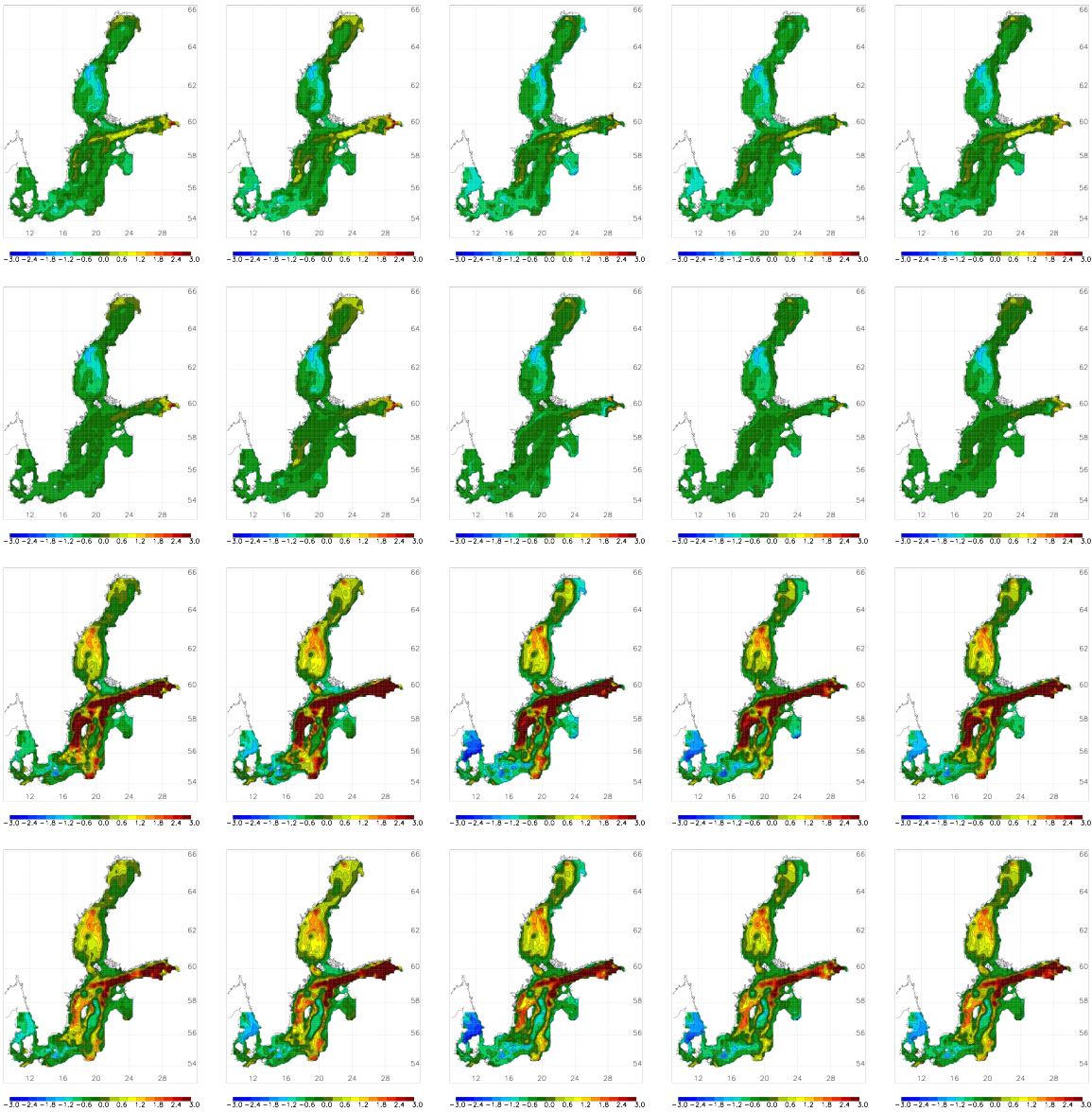


Figure 5. As Figure 1 but for bottom oxygen concentration changes (in ml l^{-1}). The color bar covers the range between -3 and +3 ml l^{-1} .

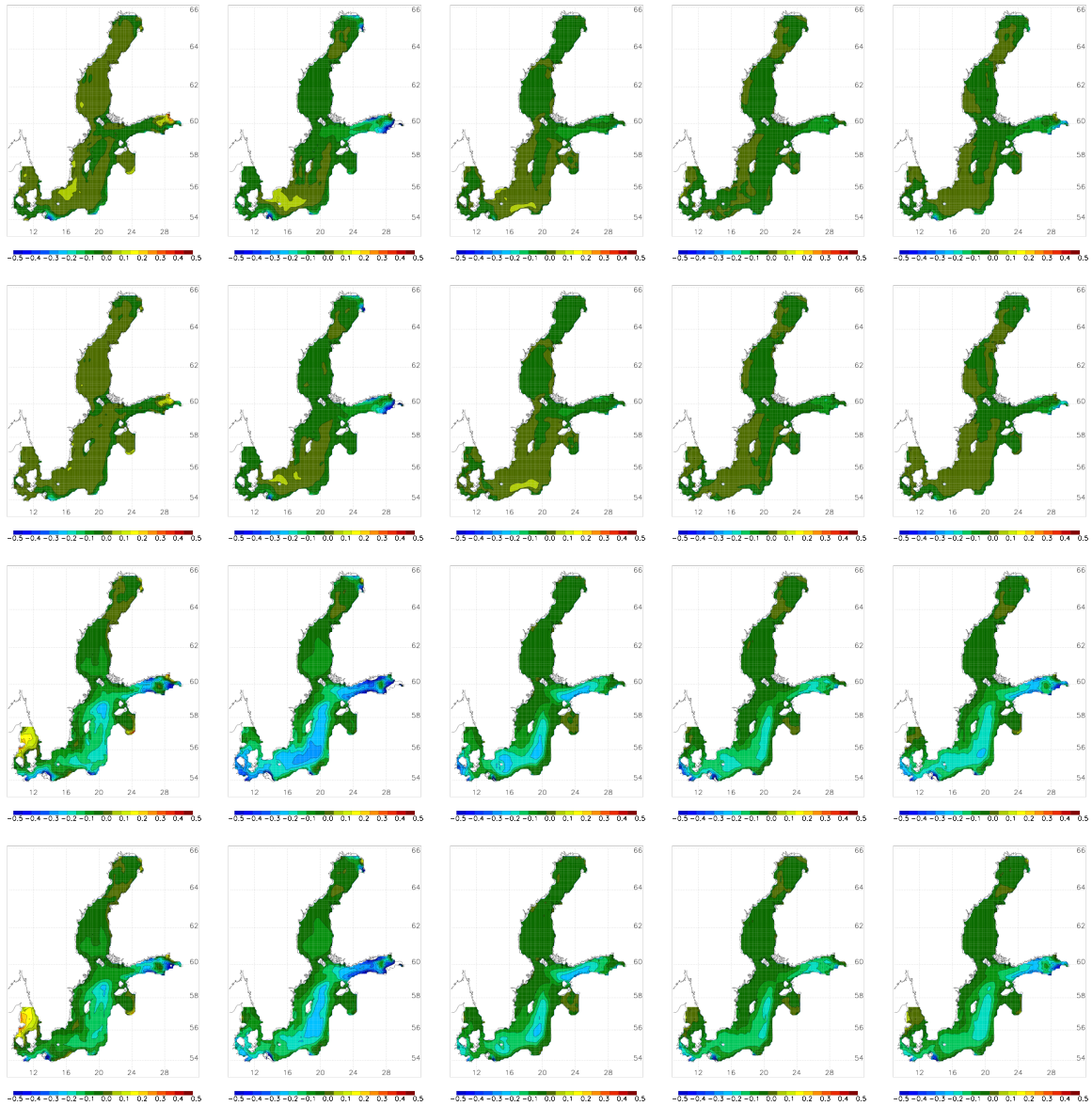


Figure 6. As Figure 1 but for phosphate concentration changes (in mmolP m^{-3}) vertically averaged for the upper 10 m. The color bar covers the range between -0.5 and $+0.5 \text{ mmolP m}^{-3}$.

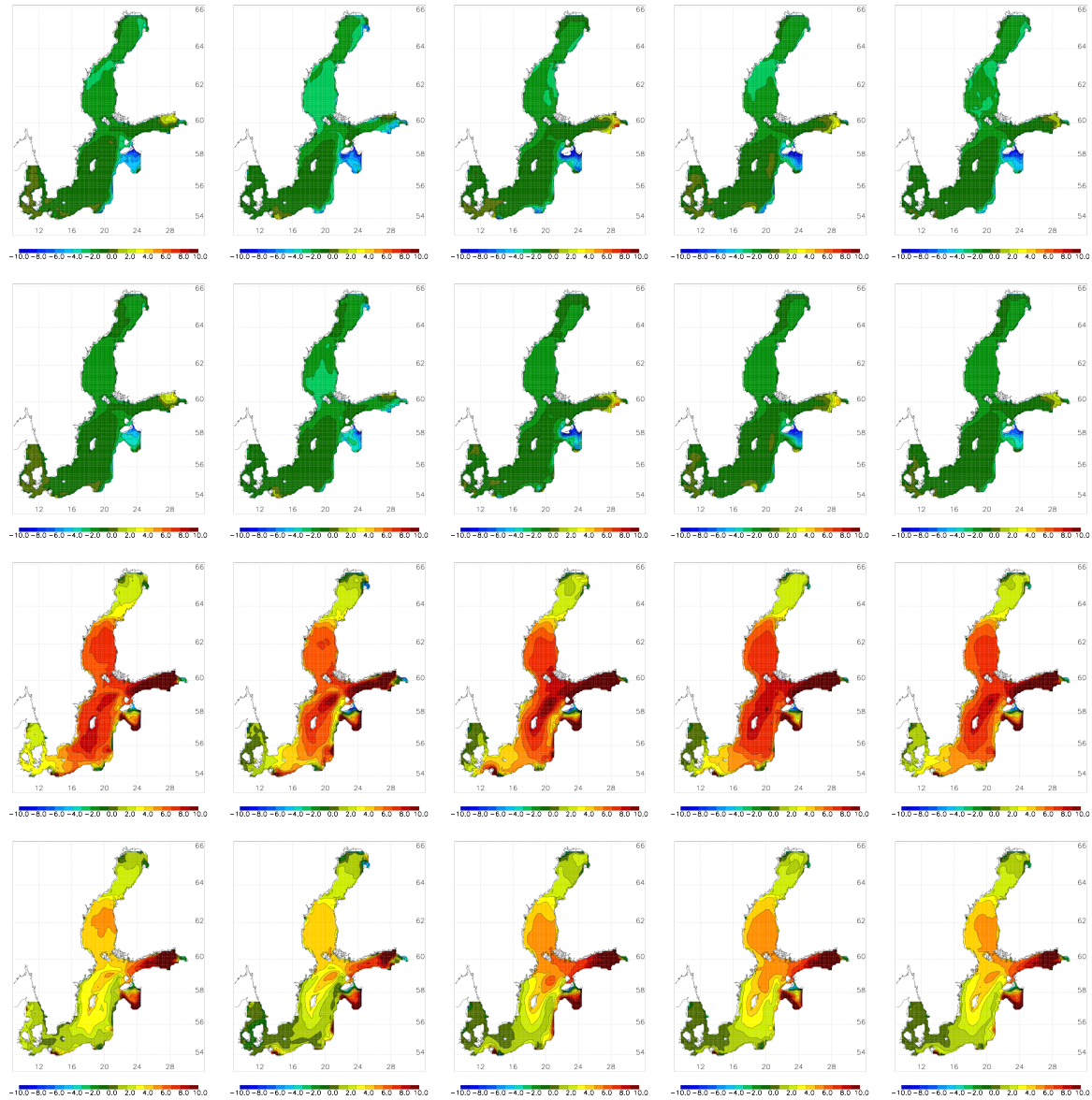


Figure 7. As Figure 1 but for nitrate concentration changes (in mmolN m^{-3}) vertically averaged for the upper 10m. The color bar covers the range between -10 and $+10 \text{ mmolN m}^{-3}$.

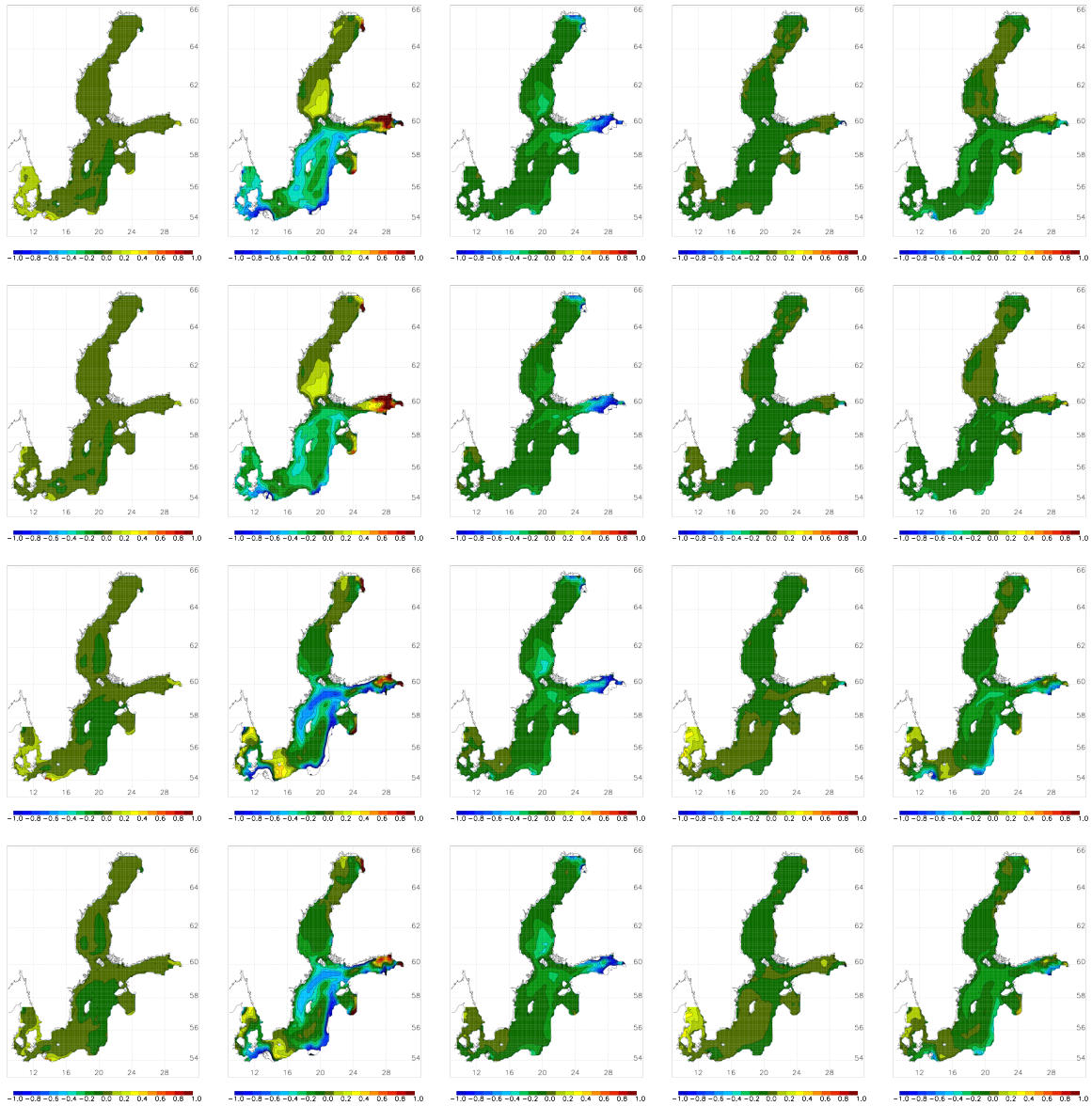


Figure 8. As Figure 1 but for diatom concentration changes (in mgChl m^{-3}) vertically averaged for the upper 10m. The color bar covers the range between -1 and +1 mgChl m^{-3} .

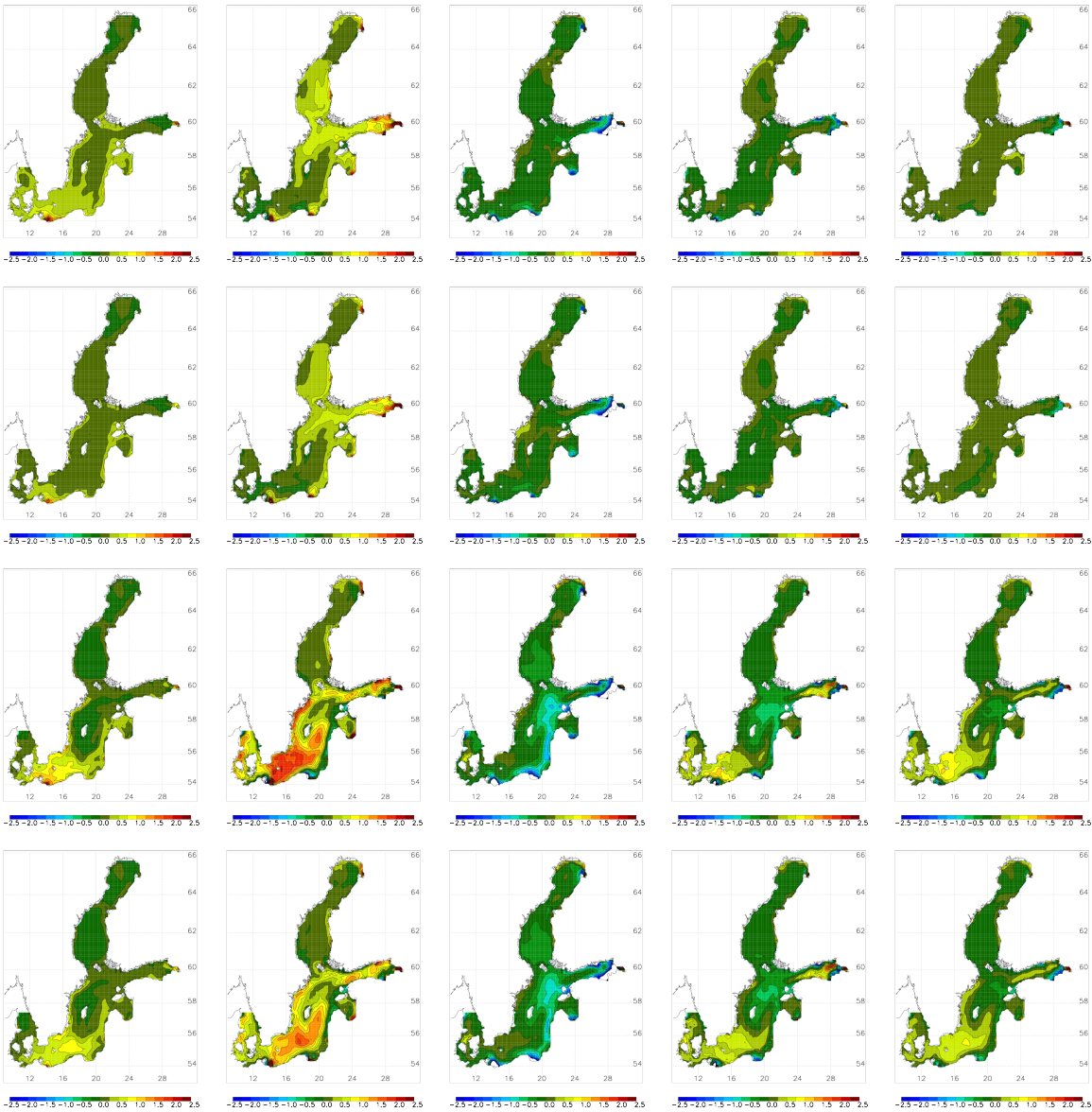


Figure 9. As Figure 1 but for concentration changes of flagellates and others (in mgChl m^{-3}) vertically averaged for the upper 10 m. The color bar covers the range between -2.5 and $+2.5 \text{ mgChl m}^{-3}$.

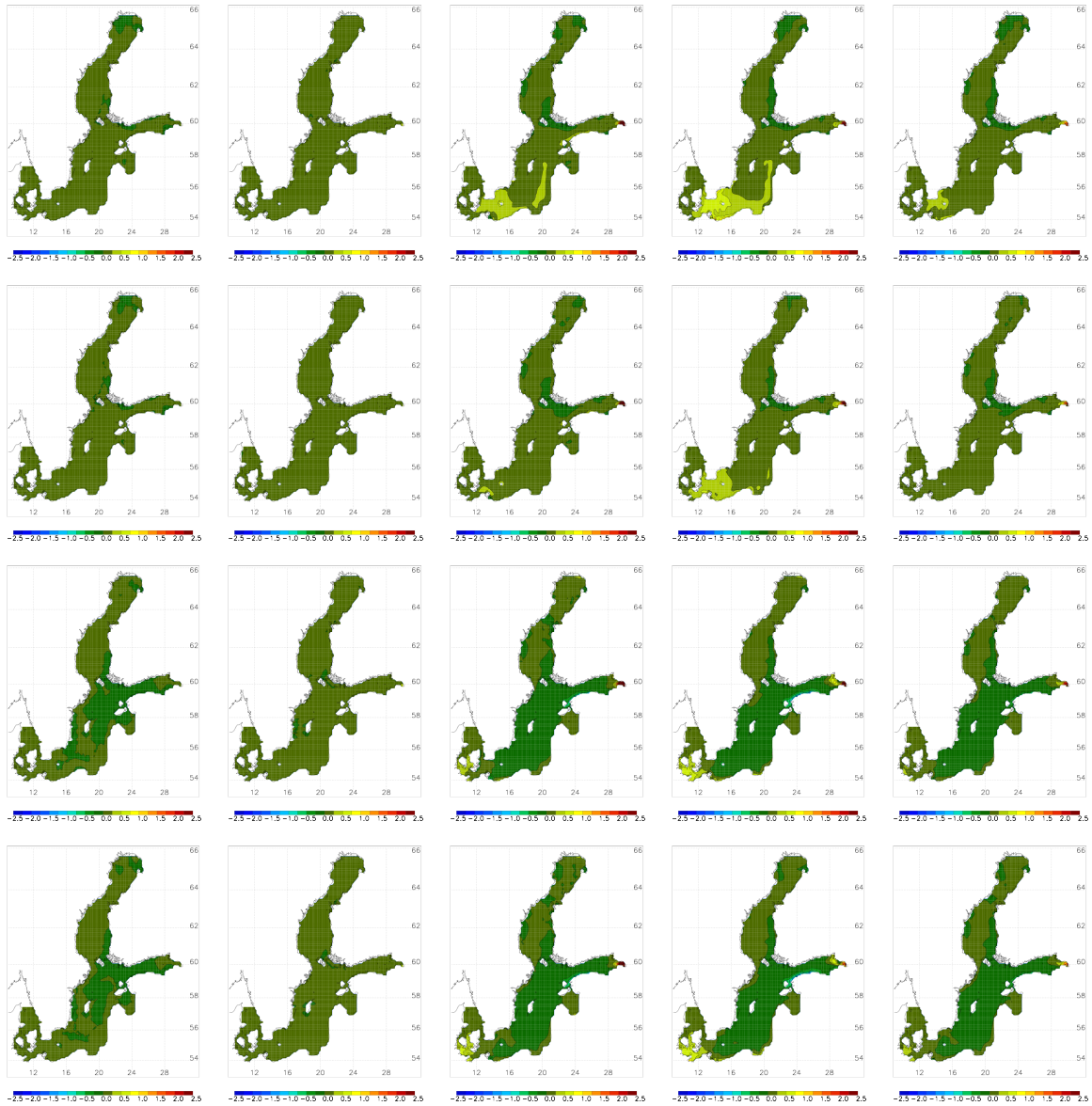


Figure 10. As Figure 1 but for cyanobacteria concentration changes (in mgChl m⁻³) vertically averaged for the upper 10m. The color bar covers the range between -2.5 and +2.5 mgChl m⁻³.

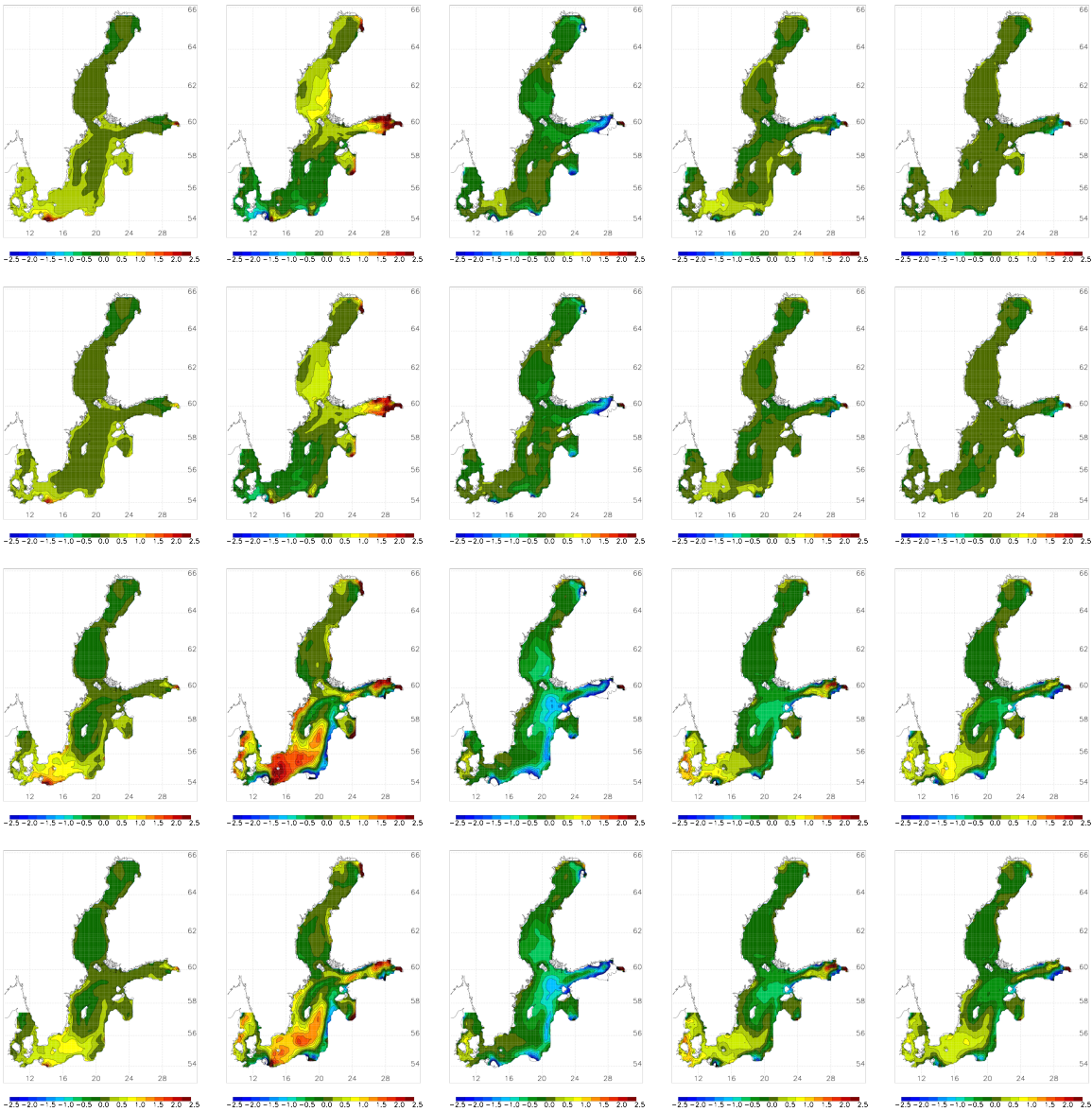


Figure 11. As Figure 1 but for phytoplankton concentration changes (in mgChl m^{-3}) vertically averaged for the upper 10m. The color bar covers the range between -2.5 and +2.5 mgChl m^{-3} .

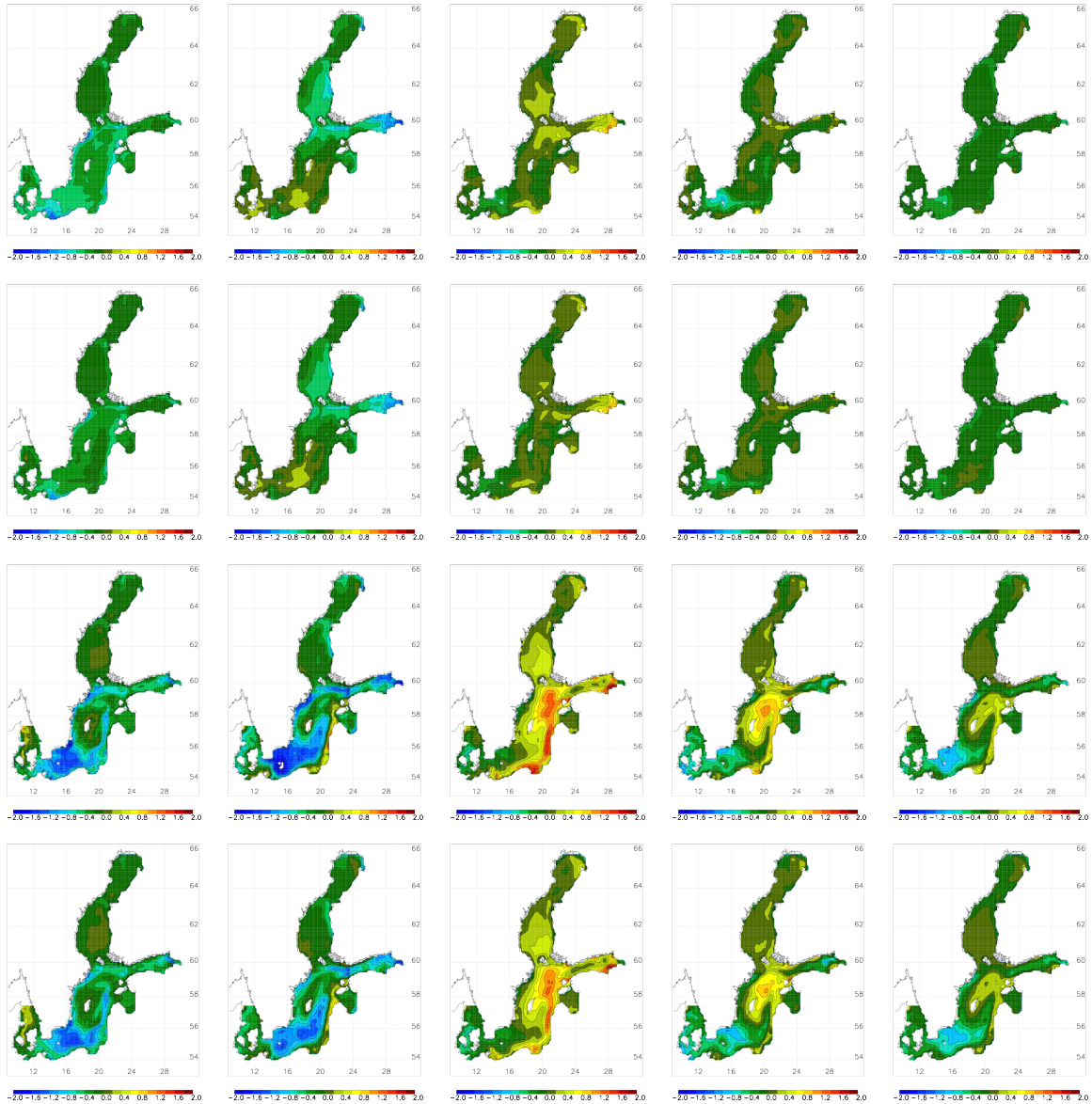


Figure 12. As Figure 1 but for secchi depth changes (in m). The color bar covers the range between -2 and +2 m.